Dynamics and stability of divacancy defects in graphene

Youngkuk Kim,[1] Jisoon Ihm,[1] Euijoon Yoon,[2,3,4,5] and Gun-Do Lee[2,*]

[1]*Department of Physics and Astronomy, Seoul National University, Seoul 151-747, Republic of Korea*

[2]*Department of Materials Science and Engineering, Seoul National University, Seoul 151-742, Republic of Korea*

[3]*Department of Nano Science and Technology, Graduate School of Convergence Science and Technology, Seoul National University, Suwon 433-270, Republic of Korea*

[4]*Department of Materials Science and Engineering, WCU Hybrid Materials Program, Seoul National University, Seoul 151-742, Republic of Korea*

[5] *Energy Semiconductor Research Center, Advanced Institutes of Convergence Technology, Seoul National University, Suwon 443-270, Korea*

(Received 4 May 2011; published 10 August 2011)

A divacancy (DV) is one of the most abundant and most important defects in irradiated graphene, which modifies electronic and chemical properties of graphene. In this paper, we present *ab initio* calculations to study the dynamics and stability of DVs in graphene. Divacancies in graphene have various reconstructed structures, such as triple pentagon-triple heptagon (555-777) and pentagon-octagon-pentagon (5-8-5) patterns. A direct observation of the structural transformations between these reconstructions was recorded in transmission electron microscope images reported by Girit *et al.* in Science **323**, 1705 (2009). We clarify the atomic structures of DVs observed in the experiment and investigate the atomic processes and energetics for the observed dynamical motions in great detail. It is found that a series of Stone–Wales-type transformations are responsible for the migration and structural transformations of DVs and that a pentagon-heptagon-heptagon-pentagon (5-7-7-5) defect appearing as an intermediate structure during the dynamical process plays an important role in the transformations of DVs.

DOI: 10.1103/PhysRevB.84.075445 PACS number(s): 61.48.Gh, 31.15.A−, 61.72.jd

I. INTRODUCTION

Since the first realization of graphene,[1–3] tremendous efforts have been made to explore its physical properties as well as the potential applications in industries. Unique properties of graphene, such as ultrahigh electron mobility,[2,4,5] high thermal conductivity,[6] and extreme mechanical properties,[7] have been examined, and it is now widely accepted that graphene is one of the most promising materials for future electronic devices. Another exciting aspect of graphene-based materials is that their exotic properties can be enriched by atomic-scale defects engineering.[8–12] Defects engineering of graphene can enormously extend the scope of applications, making graphene-based industry more plausible and promising. Indeed, chemical modifications, for example, by molecular doping[13–15] or functionalization,[16,17] are popularly suggested, and producing atomic vacancies by ionic irradiations[18,19] is also a promising way to modify properties of graphene. In particular, recently developed high-resolution transmission electron microscopy (TEM) is very useful to prove carbon-based materials. Since electron irradiation is a highly effective method to introduce various types of structural defects in graphene, many TEM studies are reported on defective graphene systems.[20,21] For example, a recent TEM study by Cretu *et al.*[22] has shown that the graphene properties can be tailored by reconstructed point defects. They have pointed out the importance of divacancies (DVs) due to their abundance at room temperature. The existence of DVs has also been predicted by other theoretical calculations showing the formation energy is lower than that of two isolated monovacancies (MVs),[23,24] and the MVs have a tendency to coalesce to a DV.[24,25]

Recently, Girit *et al.* has reported the real-time dynamics of carbon atoms in defected graphene using the aberration-corrected TEM technique.[26] The subatomic resolution of the TEM images allows the direct observation of carbon atoms in graphene and provides clear images depicting the edge structure of graphene. Furthermore, the TEM images from the supplementary movie S1 ("the TEM images" from now on) in the report happen to show various structural forms of DVs and their dynamics. These contain crucial clues to understanding the structural change of DVs. Since the dynamics of DVs and their possible control are critical issues for graphene applications, we perform first-principles calculations in this paper to provide plausible explanations for the stability and dynamics of the DV.

We first inspect the movie S1 and choose eight consecutive frames in which we presume that important information for the dynamics of DVs is recorded. Then we analyze those frames manifesting their atomic structures. Using *ab initio* computational methods, we investigate energetically favorable diffusion pathways corresponding to the dynamics observed in the frames and provide associated energy barriers. The microscopic mechanism is also provided for various types of migrations of triple pentagon-triple heptagon (555-777) and pentagon-octagon-pentagon (5-8-5) defects. Our results show 555-777 and 5-8-5 defects can migrate and rotate in the graphene plane through a sequence of Stone–Wales (SW)-type transformations. Since a specific motion of DVs has its own mechanism with distinct energy barriers, there exists a possibility to control the types of DVs produced depending on the energy of incident electrons in a TEM experiment.[27]

II. COMPUTATIONAL METHOD

The *ab initio* total energy calculations are performed with the plane-wave-basis-set VASP code[28] using a rectangular periodic supercell containing 126 carbon atoms with a single DV. The plane-wave basis is used with a kinetic energy cutoff of 400 eV. We use projector augmented wave (PAW)

potentials[29] for describing the core electrons and generalized gradient approximation (GGA) Perdew–Burke–Erenzerhof (PBE)[30] functional for the exchange correlation. In order to search the energy barrier for the SW-type transformation, which is essentially the 90° rotation of a single dimer, the orientation of the dimer is divided into small angles and fixed for one total energy calculation, while the rest atoms are fully relaxed until the force on each atom is less than 0.02 eV/Å.

III. RESULTS AND DISCUSSIONS

The TEM images in the early part of the movie[26] show the time evolution of a single DV within a suspended graphene sheet. Each frame of the TEM images is taken for 1 s of exposure with 4 s of a break. Through close inspection, we find that, starting from the fifth frame, eight sequential image frames [Figs. 1(b)–1(i)] contain meaningful evidence for the structural change of DVs, and therefore, we focus on these frames in this study. In the literature,[26] it has been reported that DVs can be reconstructed and move around in the graphene plane, owing to the kinetic energy transfer from the incident elections of 80 keV to carbon atoms.[26] The maximum energy transfer to a carbon atom has been reported to be 15.8 eV,[31] which is large enough for a DV to diffuse and change its structure in graphene, as we examine in this paper.

Figure 1 shows structural changes of DVs in a single-layer graphene from aberration-corrected TEM images. A DV is found in the region enclosed by the small (red) rectangle in Fig. 1(a). The Figs. 1(b)–1(i) show the magnified images of the region in the 5th–12th frames, respectively. Each of the fifth, seventh, and ninth frames [Figs. 1(b), 1(d), and 1(f), respectively] contains a 555-777 defect, and the 10th and 12th frames [Figs. 1(g) and 1(i)] contain a single 5-8-5 defect. The 5-8-5 defect observed in the 10th frame is different from that of the 12th frame in that the former has dangling bonds, while the latter does not. The reason that the dangling bonds remain in the former case is considered to be due to the strain by the large vacancy hole at the center or by bonds between the bottom layer and the edge of top layer, which are observed on the left-hand side of the DV structures in Fig. 1. It has been also reported that the surface of defective graphene is wrinkled, and strain is increased.[32] The two adjacent carbon atoms of each vacancy in the latter 5-8-5 defect make bonding and leave no dangling bonds. Since the structures depicted in Figs. 1(c), 1(e), and 1(h) do not correspond to any known form of metastable DV atomic structures, they can be considered to be either transient unstable structures or superposed records of metastable ones.

Atomic assignments and corresponding total charge densities obtained by *ab initio* calculations are presented in Fig. 2. The fully relaxed atomic structures are assigned in Figs. 2(a) and 2(b) with the corresponding TEM frames and the simulated total charge densities. For unstable structures in Figs. 2(c) and 2(d), we choose the atomic positions from the TEM images by assigning carbon atoms to the bright points of the image. The simulated total charge density plots show that the atomic assignments can reproduce the TEM images very well. Figure 2(h) shows the total charge density plot for the atomic structure presented in Fig. 2(d). The atomic structure is constructed from the TEM image [Fig. 1(c)] with

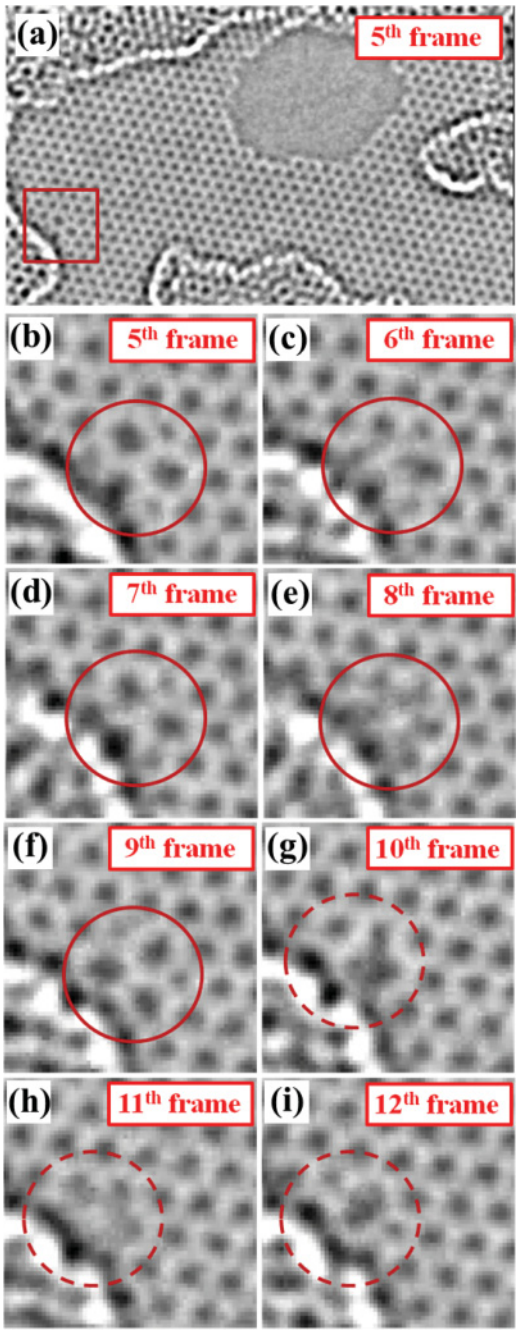

FIG. 1. (Color online) Aberration-corrected TEM images of DVs in a single-layer graphene reported in supplementary movie S1 of Ref. 26. (a) The fifth frame of the movie S1. The rectangular (red) region contains a single DV and shows various DV reconstructions. The magnified images in this region for eight consecutive frames are drawn in (b)–(i). (b) The rectangular region in the fifth frame. This frame contains a triple pentagon and triple heptagon (555-777) defect. (c) The same rectangular region of the sixth frame. (d) The seventh frame in which the 555-777 defect structure is restored. (e) The eighth frame, which captures an intermediate stage between two 555-777 defects in (d) and (f). (f) A 555-777 defect rotated by 60° with respect to the 555-777 defect in (d). (g)–(i) The 10th–12th frames. Theses frames contain a record of a single pentagon-octagon-pentagon defect (5-8-5) migration. Dashed circles in (g)–(i) are shifted one hexagon unit to the left compared to solid circles in (b)–(f) to highlight the migration of the 5-8-5 defect. Printed with the kind permission of the authors of Ref. 26.

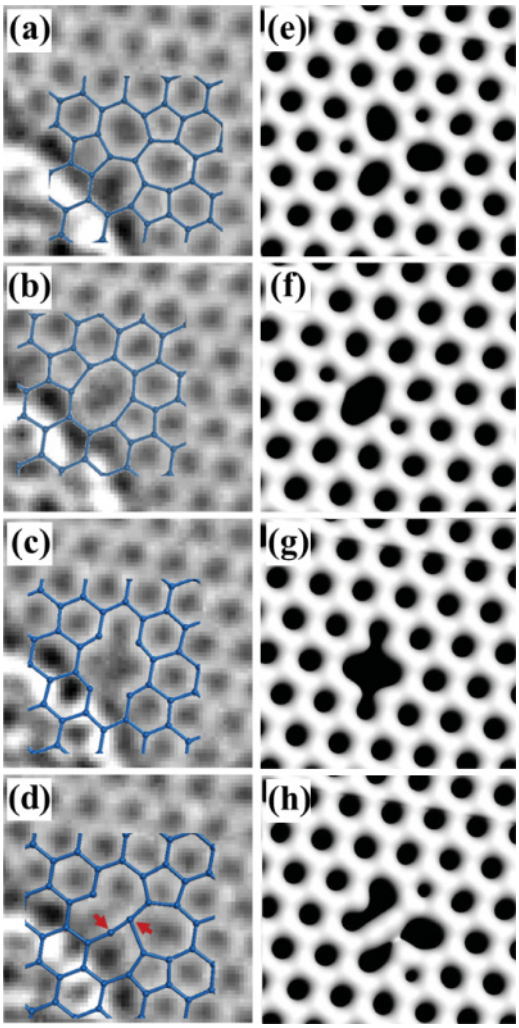

FIG. 2. (Color online) Atomic structures of DV reconstructions (a)–(d), printed with the kind permission of the authors of Ref. 26 (bars and dots are added by us for visual help), and the corresponding simulated total charge density plots (e)–(h). (a) 555-777 defect corresponding to Fig. 1(b). (b) 5-8-5 defect corresponding to Fig. 1(i). (c) 5-8-5 defect with dangling bonds corresponding to Fig. 1(g). (d) 555-777 defect with the tilted carbon dimer [corresponding to Fig. 1(c)] indicated by the two (red) arrows compared to (a). Solid (blue) bars and dots indicate their structural models. (e)–(h) Simulated total charge density plots from *ab initio* calculations for structural models of (a)–(d), respectively.

the assumption that it has a 555-777 defect with a carbon dimer tilted by about 17° [indicated by two (red) arrows in Fig. 2(d)] with respect to that of the pristine 555-777 defect [Fig. 1(b)]. The resemblance of the simulated charge density [Fig. 2(h)] to the corresponding TEM image [Fig. 1(c)] provides strong evidence for our assumption on the TEM image [Fig. 1(c)]. Therefore, the TEM image in Fig. 1(c) is analyzed to show that a carbon dimer tries to rotate by SW-type transformation but fails, and the image [Fig. 1(d)] recovers the original one [Fig. 1(b)]. As mentioned in the supplemental material of previous literature,[33] if a SW-type transformation were successful, the structural transformation between a 555-777 and a 5-8-5 defect would be observed just as shown in Figs. 1(f) and 1(g). The 555-777 defect is the most frequently observed DV structure in the TEM images (fifth, seventh, and ninth frames). With the random transfer of the kinetic energy from ejected electrons to carbon atoms during the experiment, it is natural that the more stable the structures, the more frequently they are found. Abundant appearance of 555-777 defects in the experiment is, therefore, consistent with the fact that the 555-777 defects are the most stable structures among the known DV defects.[24]

Here, we clarify the structural changes during the rotation of a 555-777 defect recorded in the 7th–9th frames of the TEM images [Figs. 1(d)–1(f)]. The 555-777 defect presented in the seventh frame [Fig. 1(d)] is recovered in the ninth frame [Fig. 1(f)] with the position of pentagons switched to that of heptagons. Therefore, it appears that the 555-777 defect experiences a rotational motion during the timespan taking the three frames (7th–9th frames). Hence, the atomic structure captured in the eighth frame [Fig. 1(e)] should record the intermediate stages of the rotation. However, since the atomic structure recorded in the frame is not matched to any known form of DVs, it is considered to be a superposition of several metastable intermediate structures. In analogy to an SW-type transformation, we propose a pathway for the rotational motion of the 555-777 defect consisting of three intermediate metastable structures: 5-8-5, pentagon-heptagon-heptagon-pentagon (5-7-7-5), and 5-8-5 defects [Figs. 3(b)–3(d)]. The 555-777 defect [Fig. 3(a)] can be transformed into a 5-8-5 defect [Fig. 3(b)] by an SW-type transformation of a carbon dimer [indicated by a dark (red) dimer in Fig. 3(a)].[24] The energy barrier for this process is found to be 6.20 eV in our *ab initio* GGA calculations, which is in good agreement with the local density approximation result (6.10 eV).[24] The energy barrier is too high to overcome by thermal activation at room temperature, and the activation energy for the transition could be provided by electron beam in TEM. The structural change of vacancy defects driven by electron beam was also addressed in detail in a very recent paper.[34] The formation energy of the 5-8-5 defect is found to be 0.93 eV higher than that of the 555-777 defect. The structural change of the 5-8-5 defect to a 5-7-7-5 defect becomes possible by the 90° rotation of the dimer (SW-type transformation), as shown in Fig. 3(b). The energy barrier for this process is 5.27 eV, as shown in Fig. 3(g). The formation energy of the 5-7-7-5 defect in Fig. 3(c) is calculated to be 4.37 eV higher than that of a 555-777 defect and 3.44 eV higher than that of a 5-8-5 defect. The 5-7-7-5 defect is not found in the original TEM images due to the high formation energy relative to the 555-777 and 5-8-5 defect structures, but it has been observed in aberration-corrected TEM images for reduced graphene oxides.[32] The 5-7-7-5 defect structure is reconstructed into the 555-777 defect through the 5-8-5 defect by two sequential SW-type transformations, as shown in Figs. 3(c)–3(e). In Fig. 3(f), we plot the average charge density of the three intermediate metastable structures (5-8-5, 5-7-7-5, and 5-8-5 defects). In the charge density plot, a white spot area appears at the position of the center of two 555-777 defects, and it is surrounded by six dark spots, which are located with an angular interval of 60° each. The figure shows a quite good agreement with the TEM image in the eighth frame [Fig. 1(e)]. Especially the position of the darker spot on the right-hand side among those six dark spots is in excellent agreement with the

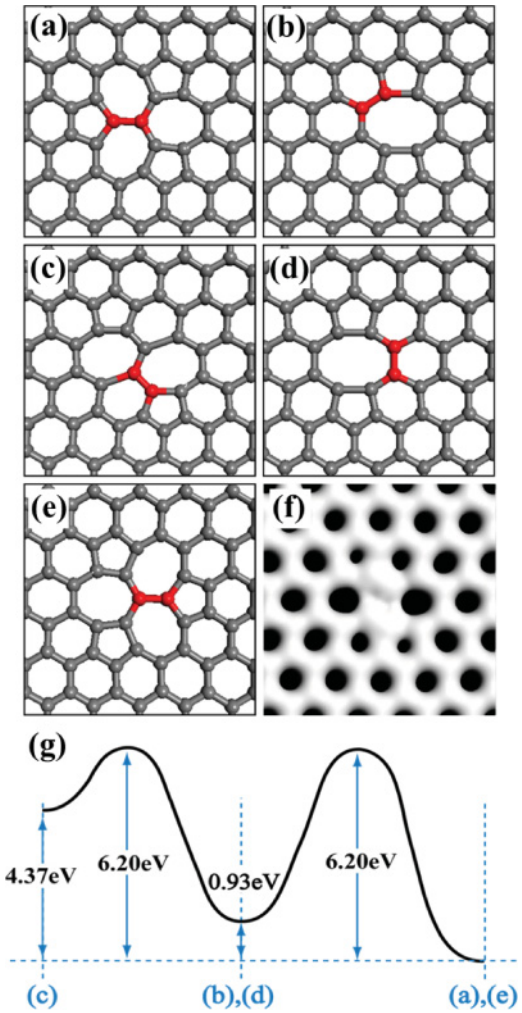

FIG. 3. (Color online) Microscopic atomic process for the rotational motion of a 555-777 defect. (a) 555-777 defect. (b) 5-8-5 defect. (c) 5-7-7-5 defect. (d) 5-8-5 defect. (e) 555-777 defect. (f) The charge density plot obtained by averaging the three intermediate structures, (b)–(d). (g) Energy barriers for this process and formation energies relative to the 555-777 defect. Atomic structures shown in (b)–(e) can be obtained by a SW transformation of the dark (red) dimer shown in (a)–(d), respectively.

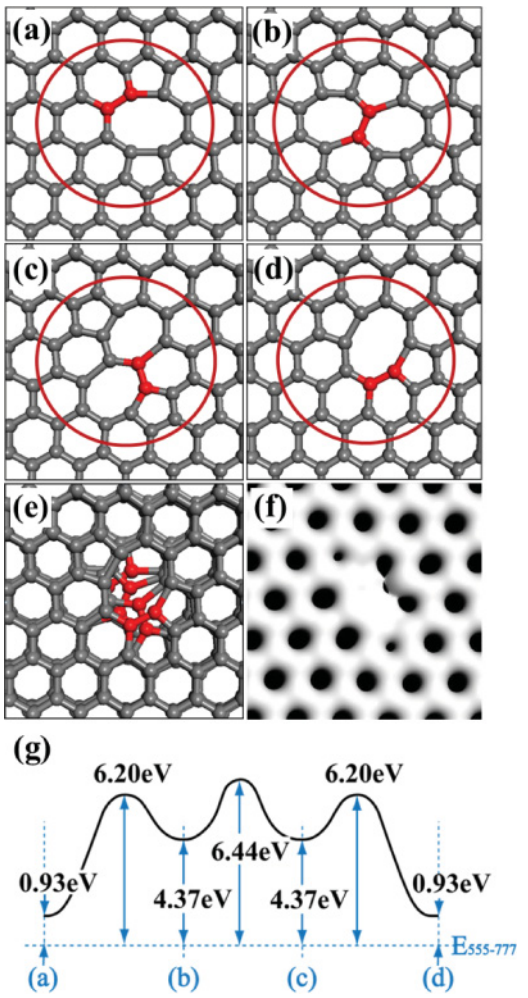

FIG. 4. (Color online) Microscopic atomic process for the migration of a 5-8-5 defect. (a) 5-8-5 defect corresponding to the TEM image in Fig. 1(g). (b) 5-7-7-5 defect. (c) 5-7-7-5 defect. (d) 5-8-5 defect. The atomic structure in (d) corresponds to the atomic assignment of Fig 1(i). Dark (red) dimer in each figure is the part which undergoes an SW-type transformation. (e) Superposition of the atomic structures, (a)–(d). (f) The simulated total charge density plot obtained by averaging the four structures, (a)–(d). (g) Schematic diagram representing energy barriers for the 5-8-5 migration from (a) to (d) and formation energies relative to the 555-777 defect.

position of the larger dark spot in Fig. 3(f). The resemblance of the charge density to the TEM image in the eighth frame provides reasonable evidence for our interpretation. Although we consider another pathway of direct transformation from Fig. 3(a) to Fig. 3(e) by the simultaneous 60° rotation of three carbon atoms around the center atom of the 555-777 defect structure, the energy barrier is found to be higher than that of our favorable pathway by 1.7 eV.

We also investigate the migration of a 5-8-5 defect recorded in 10th–12th frames of the original TEM images [Figs. 1(g)–1(i)]. As previously mentioned, the DV defects appearing in the 10th and 12th frames are different kinds of 5-8-5 defects; the 5-8-5 defect in the 10th frame [Fig. 1(g)] has dangling bonds, while the other does not [Fig. 1(i)]. For the present discussion on the migration of a 5-8-5 defect, however, we only consider 5-8-5 defects without dangling bonds because the dangling bonds disappear easily in the structural relaxation of 5-8-5 defects according to our *ab initio* calculations. The intermediate 11th frame shows an unclear atomic configuration, and it is also conjectured to be a superposition of intermediate metastable structures. As shown in Figs. 4(a)–4(d), the 5-8-5 defect structure undergoes the migration and the 60∞ rotation via 5-7-7-5 defects twice by three sequential SW-type transformations. The corresponding energy barriers for the pathway are shown in Fig. 4(f). The structural transition is also considered to be due to the electron irradiation from TEM because the energy barrier is too high to overcome just by thermal activation at room temperature. The superposition of the two 5-8-5 defects [Figs. 4(a) and 4(d)] and two 5-7-7-5 defects [Figs. 4(b) and 4(c)] structures and the average of their simulated total charge densities are shown in Figs. 4(e) and 4(f), respectively. The average charge density plot shows charge deficiency between two black spots in the upper right-hand direction

from the center of the defects. This is in quite good agreement with the TEM image in the 11th frame [Fig. 1(h)]. Therefore, the 11th frame is considered to be a superposition of those metastable structures. Our analysis again indicates that the rotation of the 5-8-5 defect found in the TEM images may be achieved by a series of SW-type transformations.

IV. SUMMARY

We have investigated the dynamics and stabilities of DVs in graphene observed in the TEM experiment by *ab initio* total energy calculations. The TEM images reported in the literature[26] contain various DV reconstruction structures, such as 555-777 and 5-8-5 defects, providing evidence for the structural transformations among those DVs. We have calculated detailed microscopic process of the 555-777 rotation as well as the 5-8-5 migration and corresponding energy landscapes. In the structural transformation of DVs, the 5-7-7-5 defect is found to play an important role as a metastable structure. Our simulated images are in good agreement with the observed TEM pictures, and these results provide a deep insight into the dynamics of DVs in graphene.

ACKNOWLEDGMENTS

This work was supported by the Basic Science Research Program through the National Research Foundation of Korea funded by the Ministry of Education, Science and Technology (No. 2011-0000904, 2010-0012670 and KRF-2006-341-C000015) and the Core Competence Enhancement Program of KIST through the Hybrid Computational Science Laboratory. The authors also acknowledge the support from KISTI under the Supercomputing Applications Support Program. This research was also supported by the World Class University program through National Research Foundation of Korea funded by the Ministry of Education, Science and Technology (R31-2008-000-10075-0). The authors acknowledge the authors of Ref. 26 for their kind permission to print their data. Some figures reprinted with permission from AAAS.

*Corresponding author: gdlee@snu.ac.kr

[1] K. S. Novoselov, A. K. Geim, S. V. Morozov, D. Jiang, Y. Zhang, S. V. Dubonos, I. V. Grigorieva, and A. A. Firsov, Science **306**, 666 (2004).
[2] K. S. Novoselov, A. K. Geim, S. V. Morozov, D. Jiang, M. I. Katsnelson, I. V. Grigorieva, S. V. Dubonos, and A. A. Firsov, Nature **438**, 197 (2005).
[3] Y. B. Zhang, Y. W. Tan, H. L. Stormer, and P. Kim, Nature **438**, 201 (2005).
[4] S. V. Morozov, K. S. Novoselov, M. I. Katsnelson, F. Schedin, D. Elias, J. A. Jaszczak, and A. K. Geim, Phys. Rev. Lett. **100**, 016602 (2008).
[5] J. H. Chen, C. Jang, S. Xiao, M. Ishigami, and M. S. Fuhrer, Nat Nano **3**, 206 (2008).
[6] A. A. Balandin, S. Ghosh, W. Bao, I. Calizo, D. Teweldebrhan, F. Miao, and C. N. Lau, Nano Lett. **8**, 902 (2008).
[7] C. Lee, X. Wei, J. W. Kysar, and J. Hone, Science **321**, 385 (2008).
[8] P. O. Lehtinen, A. S. Foster, A. Ayuela, A. Krasheninnikov, K. Nordlund, and R. M. Nieminen, Phys. Rev. Lett. **91**, 017202 (2003).
[9] K. T. Chan, J. B. Neaton, and M. L. Cohen, Phys. Rev. B **77**, 235430 (2008).
[10] X. R. Wang, X. L. Li, L. Zhang, Y. Yoon, P. K. Weber, H. L. Wang, J. Guo, and H. J. Dai, Science **324**, 768 (2009).
[11] C. Coletti, C. Riedl, D. S. Lee, B. Krauss, L. Patthey, K. von Klitzing, J. H. Smet, and U. Starke, Phys. Rev. B **81**, 235401 (2010).
[12] O. C. Compton and S. T. Nguyen, Small **6**, 711 (2010).
[13] T. O. Wehling, K. S. Novoselov, S. V. Morozov, E. E. Vdovin, M. I. Katsnelson, A. K. Geim, and A. I. Lichtenstein, Nano Lett. **8**, 173 (2007).
[14] H. Liu, Y. Liu, and D. Zhu, J. Mater. Chem. **21**, 3335 (2011).
[15] F. Schedin, A. K. Geim, S. V. Morozov, E. W. Hill, P. Blake, M. I. Katsnelson, and K. S. Novoselov, Nat. Mater. **6**, 652 (2007).
[16] D. W. Boukhvalov and M. I. Katsnelson, J. Phys. Condens. Matter **21**, 344205 (2009).
[17] S. Gowtham, R. H. Scheicher, R. Ahuja, R. Pandey, and S. P. Karna, Phys. Rev. B **76**, 033401 (2007).
[18] O. Lehtinen, J. Kotakoski, A. V. Krasheninnikov, and J. Keinonen, Nanotechnology **22**, 175306 (2011).
[19] A. V. Krasheninnikov and F. Banhart, Nat Mater **6**, 723 (2007).
[20] F. Banhart, J. Kotakoski, and A. V. Krasheninnikov, ACS Nano **5**, 26 (2010).
[21] A. Hashimoto, K. Suenaga, A. Gloter, K. Urita, and S. Iijima, Nature **430**, 870 (2004).
[22] O. Cretu, A. V. Krasheninnikov, J. A. Rodriguez-Manzo, L. Sun, R. M. Nieminen, and F. Banhart, Phys. Rev. Lett. **105**, 196102 (2010).
[23] M. Saito, K. Yamashita, and T. Oda, Jpn. J. Appl. Phys. **46**, L1185 (2007).
[24] G. D. Lee, C. Z. Wang, E. Yoon, N. M. Hwang, D. Y. Kim, and K. M. Ho, Phys. Rev. Lett. **95**, 205501 (2005).
[25] A. V. Krasheninnikov, P. O. Lehtinen, A. S. Foster, and R. M. Nieminen, Chem. Phys. Lett. **418**, 132 (2006).
[26] Ç. Ö. Girit, J. C. Meyer, R. Erni, M. D. Rossell, C. Kisielowski, L. Yang, C.-H. Park, M. F. Crommie, M. L. Cohen, S. G. Louie, A. Zettl, Science **323**, 1705 (2009).
[27] J. Kotakoski, A. V. Krasheninnikov, U. Kaiser, and J. C. Meyer, Phys. Rev. Lett. **106**, 105505 (2011).
[28] G. Kresse and J. Furthmuller, Comput. Mater. Sci. **6**, 15 (1996).
[29] P. E. Blöchl, Phys. Rev. B **50**, 17953 (1994).
[30] J. P. Perdew, K. Burke, and M. Ernzerhof, Phys. Rev. Lett. **78**, 1396 (1997).
[31] B. W. Smith and D. E. Luzzi, J. Appl. Phys. **90**, 3509 (2001).
[32] C. Goómez-Navarro, J. C. Meyer, R. S. Sundaram, A. Chuvilin, S. Kurasch, M. Burghard, K. Kern, and U. Kaiser, Nano Lett. **10**, 1144 (2010).
[33] G. D. Lee, C. Z. Wang, E. Yoon, N. M. Hwang, and K. M. Ho, Phys. Rev. B **81**, 195419 (2010).
[34] J. Kotakoski, J. C. Meyer, S. Kurasch, D. Santos-Cottin, U. Kaiser, and A. V. Krasheninnikov, Phys. Rev. B **83**, 245420 (2011).